doi:10.1017/S1431927622006092
Microsc. Microanal. 28 (Suppl 1), 2022

Three-dimensional Structural Analysis of Ant Hair Sensors by X-ray and Serial Block-Face Scanning Electron Microscope Imaging

Lei Gao[1], Yang Yu[2], Zixiong Cao[3] and Yalin Wang[1*]

[1.] Microscopy Core Facility, Westlake University, Hangzhou, Zhejiang, China
[2.] Carl Zeiss (Shanghai) Co., Ltd, Shanghai, China
[3.] Object Research Systems (ORS), Inc., Quebec, Canada.
* Corresponding author: wangyalin@westlake.edu.cn

Abstract: Traditional methods of studying ant hair sensors relied on empirical experience and semi-thin sectioning for localization of the structures, but it was very difficult to obtain the 3D structure of a complete sensor at EM level. Here we describe an approach for 3D structural analysis of ant sensors using state-of-the-art X-ray microscope and serial block-face scanning electron microscope (SBF-SEM). We selected 1/4 of the ant head (Fig.A) and processed it using the rOTO method. After embedding in Epon 812，the sample was scanned with a Versa 510 X-Ray microscope (XRM-510, Zeiss) to find the sensors. Then the target sensors were scanned at a higher resolution. The X-Ray data sets were used for reference to direct subsequent trimming. A semi-thin section was cut and compared with a virtual X-ray section to align the resin block with the X-ray data set. One ant hair sensor about 360 μm below the block surface was chosen for current analysis. About 355 μm-thick material above the sensor was removed by serial semi-thin sectioning at 200 nm intervals. The last section was compared side-by-side with a virtual slice from the X-Ray of higher resolution. After precisely locating the sensor, the sample was further trimmed into a cube of 100 μm × 130 μm × 200 μm and mounted on an SBF-SEM pin, sputter coated with 50 nm palladium, and imaged using a Gemini scanning electron microscope (Zeiss) equipped with 3View/2XP and OnPoint backscatter detector (Gatan). The alignment, segmentation, and reconstruction of acquired images were carried out using Dragonfly Pro software (Object Research Systems). 3D-reconstruction of the sensor was performed by manual segmentation of the indicated subcellular compartments.

Samples typically processed for serial block-face imaging can be scanned with the X-ray microscope and regions of interest quickly identified, avoiding time-consuming searches of regions of interest with semi-thin sectioning. This allows targeted trimming, and thus greatly facilitates the preparation of resin blocks for serial block-face imaging and image acquisition [6].

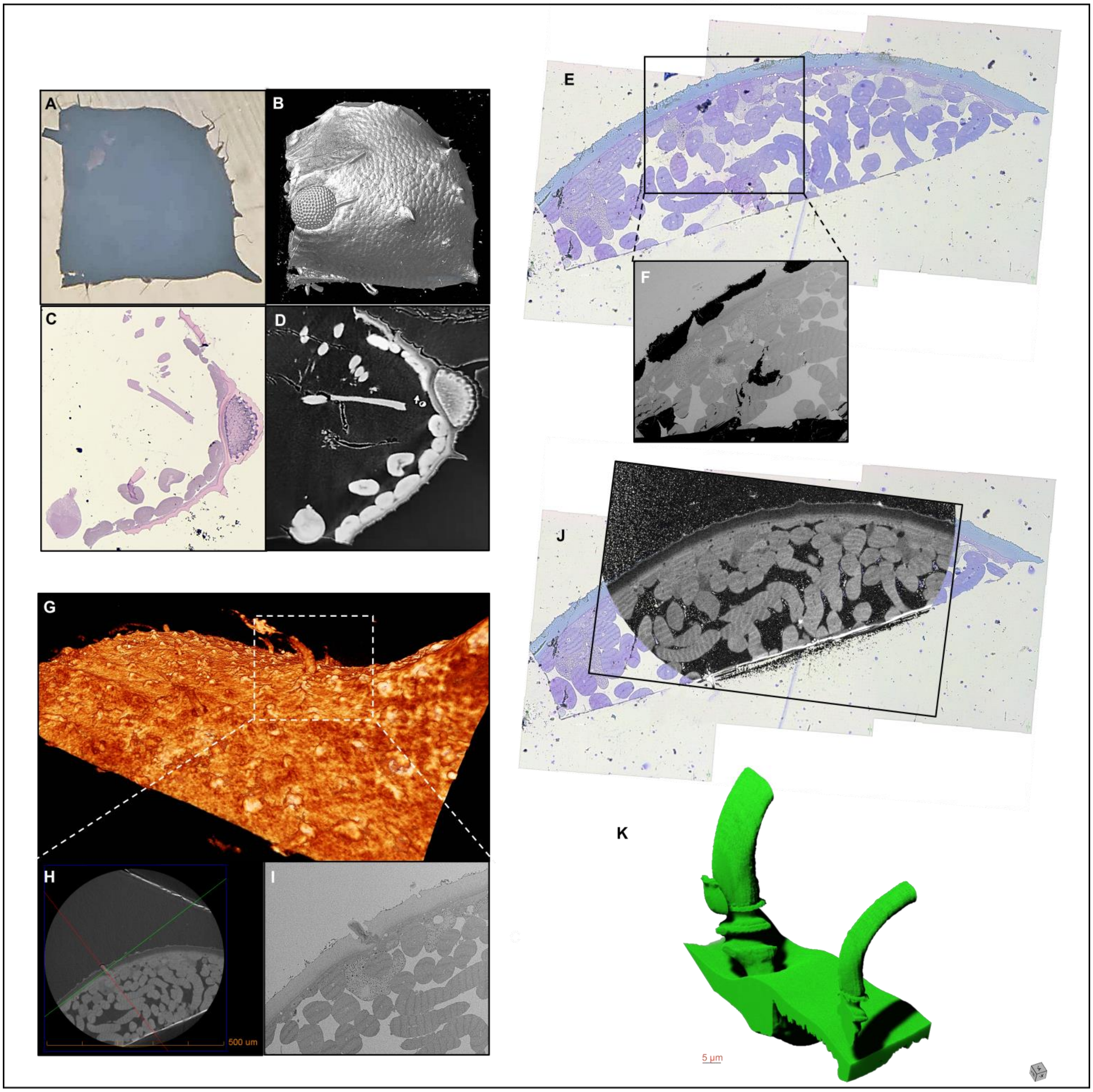

Figure 1. Fig.A The resin-embedded sample seen under a light microscope. Fig.B Surface rendering of the X-ray tomogram (acquired on a Zeiss Versa 510) of the resin-embedded ant head. Fig.C-D Alignment of the resin block on the ultramicrotome with the X-ray tomogram. A semi-thin (200nm) section was cut (Fig.C) and matched with a virtual section of the X-ray tomogram (Fig.D). The target sensor lies about 360µm below the block surface. Fig.E-F Matching of the semi-thin section (Fig.E) with the virtual slice from the X-ray tomogram (Fig.F) after removing 355µm-thick material from the resin block. Fig.G Surface rendering of an X-ray tomogram showing the area with the target sensor. Fig.H A

https://doi.org/10.1017/S1431927622006092 Published online by Cambridge University Press

virtual X-ray slice of the sensor (boxed area in Fig.G) at 386.3 μm below the block surface. Fig.I The same region imaged with SBF-SEM. The trimmed sample was sliced repeatedly, removing 50nm-thick material at each cut. Each newly-exposed surface was imaged in the target sensor area, using an SEM beam at 1.5 keV with a dwell time of 0.8 μs/pixel and a pixel size of 15 nm. Focal Charge Compensation (FCC) at 10% was used to eliminate specimen charging. 682 serial images were collected. Fig.J SBF-SEM image of the target area after further removal of 1um of materials matched with the last semi-thin section. Fig.K Volume rendering of the target sensor. importing into the document. Check that the line widths and font sizes allow the figure to be clear at its final size.

References:

[1] Feng-Xia Liang et al., Microscopy Today, Volume 29, Issue 1, January 2021, pp. 18 – 23. doi.org/10.1017/S1551929520001777.
[2] Tobias Starborg et al., Ultramicroscopy, Volume 201, June 2019, Pages 58-67. doi.org/10.1016/j.ultramic.2019.03.002Get rights and content
[3] Alexey A. Polilov et al., Sci Rep 11, 4717 (2021). doi.org/10.1038/s41598-021-83936-0.
[4] Tin Ki Tsang et al., eLife 2018;7:e35524 DOI: 10.7554/eLife.35524.
[5] Clarisse Uwizeye et al., Nature communications, (2021) 12:1049, doi.org/10.1038/s41467-021-21314-0.
[6] The authors acknowledge funding from the National Natural Science Foundation of China (Nos. 8190080864) and Westlake University Core Facility Development Fund, Dr. Lin Li is thanked for his many useful discussions and contributions to this work.